Applications of density functional theory to heavy metal binding to magnetic-cored dendrimer

IOP Conf. Series: Materials Science and Engineering **615** (2019) 012067 doi:10.1088/1757-899X/615/1/012067

Applications of density functional theory to heavy metal binding to magnetic-cored dendrimer

H-R Kim[1], D W Boukhvalov[2] and J-W Park[1*]

[1] Department of Civil and Environmental Engineering, Hanyang University, 222 Wangsimni-ro, Seongdong-gu, Seoul 04763, South Korea
[2] Department of Chemistry, Hanyang University, 222 Wangsimni-ro, Seongdong-gu, Seoul 04763, South Korea

[*]Corresponding author e-mail: jaewoopark@hanyang.ac.kr

Abstract. Magnetic-cored dendrimer (MD) is a nano-material composed with the magnetite nanoparticle in the core and dendritic branches developed on the surface of the core. Due to the unique structure and magnetic property of the MD, it has been studied for various environmental applications including the adsorption. With a large number of the terminal group, the poly (amidoamine) dendrimer provides many possible binding positions to various kind of contaminants. It has been reported that the heavy metal adsorption shows different affinity depending on heavy metal species in the aqueous phase. In this study, the MD was synthesized and their binding efficiency experimented with four different dissolved heavy metals of Pb (II), Cu (II), Zn (II), and Cr (VI). The maximum adsorption capacity of heavy metal was in the following order: $Pb^{2+} > HCrO_4^- > Zn^{2+} > Cu^{2+}$. The interaction between the MD and the targeted heavy metal was calculated using the density functional theory (DFT). A pseudo-potential code SIESTA model was used. The calculated enthalpy of each metal indicated an agreement with the experimental result. A specific binding position and energies of different heavy metal species were confirmed through DFT calculations. The calculated enthalpy demonstrates structural and dynamical characteristics between MD and heavy metals. The binding preference of MD to a different kind of heavy metal provides useful information for the environmental applications.

1. Introduction

One of the advantages of dendrimer is that it can control the number of terminal groups by generation growth [1-3]. The generation growth of dendrimer can enhance the reactivity to the target material [4]. Magnetic-cored dendrimer (MD) is one of the outstanding combinations for easier separation and more dendritic branches [5-6]. Since the dendritic branches of MD are grown on the surface on the MNP, the number of the functional group is greater than normal PAMAM dendrimer, which has ethylenediamine as a core. The MD of about 9 nm has 748 of 3-aminopropyl trimethoxysilane (APTS) on their surface area [7]. With a large number of sorptive sites in MD, the removal efficiency is expected to be improved along with facile separation.

In this work, we selected four different heavy metal species to estimate the binding capacity onto G1-MD. The three metal ions of Pb (II), Cu (II), and Zn (II) exist in the di-valent (2+) but have different ionic radius and electronegativity. Cr(VI) is negatively charged in the aqueous phase, so the adsorption affinity can be different [8]. Experimental results were interpreted through computational calculation

using the density functional theory (DFT) method. The calculation result enables to understand the optimal configuration of each metal species on dendritic structure. The results from the DFT applications provides essential information on interfaces, and it enables to predict the molecular relations of the systems [9].

2. Experiments

2.1. Materials

Iron (II) sulfate heptahydrate, zinc chloride, potassium dichromate, copper (II) sulfate pentahydrate, 3-aminopropyl trimethoxysilane (APTS), and lead (II) nitrate were purchased from Sigma-Aldrich (USA). Sodium hydroxide was purchased from Showa (Japan). Ethylenediamine anhydrous and ammonium hydroxide were purchased from Daejung Chemicals & Metals (Korea). Iron (III) chloride hexahydrate, methyl acrylate, and hydrochloric acid were purchased from Junsei Chemical (Japan). Methyl alcohol was purchased from Samchun Chemical (Korea).

2.2. Preparation of G1-MD

Magnetic nanoparticle (MNP), APTS modified magnetic-cored dendrimer (G0-MD), and G1-MD was prepared following the procedures. Ammonium hydroxide solution added into the mixture of iron (II) sulfate heptahydrate and iron (III) chloride hexahydrate solution for MNP formation. Dendritic structure was formed through successive reactions with APTS, methyl acrylate, and ethylenedimaine. The MNP was dispersed in the methanol and 25 ml of APTS was added. The solution was agitated for 7 hours at 60 ℃. Synthesized G0-MD were reacted with 50 ml of methylacrylate at room temperature for 7 hours. Then, 10 ml of EDA was added into G0-MD and agitated at room temperature for 3 hours to prepare G1-MD. The prepared materials were washed using methanol for five times each.

2.3. Characterization

Transmission electron microscopy (TEM, JEM-2010, JEOL, Japan) was used to observe the morphology of the final product. The X-ray diffraction (XRD) patterns were characterized using an X-ray diffractometer (Rigaku D/MAX RINT 2000, Japan) with Cu Kα radiation (λ = 1.5418740 Å). Specific surface area and pore size distribution were measured using the surface area analyzer (Autosorb-iQ 2ST/MP, Quantachrome, USA) using Brunauer–Emmett–Teller (BET) N_2 method. The concentration of heavy metal ions in the solution was analyzed with the inductive coupled plasma optical emission spectrometer (ICP-OES, Optima ICP-OES 8000, Perkin Elmer, USA).

2.4. Adsorption experiment and computational calculation

Adsorption experiment was performed at a room temperature in batch mode. A fixed mass of adsorbent (0.03g) was added into 30 ml of heavy metal solutions. The pH was adjusted to 5 for Pb^{2+}, Cu^{2+}, and Zn^{2+} and 2 for $HCrO_4^-$ using 0.01M of NaOH and HCl, respectively. Kinetic experiment was performed using 20 mg/ L of initial concentration for each metal species. Heavy metal solutions with the concentration range of 10 to 400 mg/ L were used for equilibrium experiment. After the adsorption, the mixture was placed on a magnet for 10 min and the supernatant was filtered through a 0.45 μm syringe filter. The concentration of the supernatants was analyzed using ICP-OES.

A DFT calculation was used to demonstrate the molecular interaction between G1-MD and targeted metal species. A pseudo-potential code, SIESTA model was used in this research [10]. The calculations were conducted using the generalized gradient approximation (GGA-PBE) with spin-polarization. We performed the calculation of dendritic branches attached to the MNP surface. The DFT-based 0 K adsorption enthalpy was calculated as follows:

$$\Delta H_{ab}=[(E_{host+guest})-(E_{host}+E_{guest})]/N \quad (1)$$

where $E_{host+guest}$ is the total energy of G1- MD system before adsorption with the adsorbed N guest atoms, E_{host} is the total energy of a pure G1- MD system, while E_{guest} is the energy of the guest's ion.

2.5. Characterization

Morphology of G1-MD was confirmed by TEM image shown in figure 1 (a). A well-defined global structure was confirmed and the particle's size was about 10-12 nm. The XRD data shows that the MNP and G1-MD have magnetite crystal form (ICDD 01-071-6336) which possess paramagnetic property. No significant difference was observed after the dendritic structure formation on the MNP surface (see figure 1 (b)). Nitrogen sorption-desorption onto MNP, G0-MD, and G1-MD are shown in figure 2. The hysteresis loops of each product were classified as type-IV, and indicate the presence of mesoporous pores with a relatively high pore-size uniformity [11, 12]. The BET surface areas of MNP, G0-MD, and G1-MD were 99.2 m^2 g^{-1}, 96.6 m^2 g^{-1}, and 101.4 m^2 g^{-1}, respectively.

2.6. Adsorption experiment

The kinetic results in figure 3 indicate that an equilibrium was reached within 60 min. Both Pb^{2+} and $HCrO_4^-$ adsorption kinetics were better fitted with a pseudo-second-order kinetic model compared to the pseudo-first-order model. This indicates that the binding mechanism of the G1-MD and heavy metal ions predominantly corresponded to chemisorption [4]. Equilibrium isotherm parameters were shown in table 1. The Langmuir isotherm can be expressed as follows:

$$\frac{C_e}{q_e} = \frac{1}{K_L q_0} + \frac{C_e}{q_0} \tag{2}$$

where Ce is the equilibrium concentration of heavy metal ions in the solution (mg L^{-1}), qe is the adsorbed value of heavy metal ions at the equilibrium concentration (mg g-1), q_0 is the maximum adsorption capacity (mg g^{-1}), and K_L is the Langmuir constant. Langmuir isotherm model was well-fitted to the experimental values. The maximum adsorption capacity of G1-MD shows the highest value in Pb^{2+} adsorption. Below pH 5, dominant species of Cr (IV) is $HCrO^{4-}$ and electrostatic interaction is derived between $HCrO^{4-}$ and the positively charged surface of the adsorbent. The binding preference onto the G1-MD was identified in the mixed system of Pb^{2+}, Cu^{2+}, and Zn^{2+} in pH 5.0. In figure 4, the adsorption affinity of Pb^{2+}, Cu^{2+}, and Zn^{2+} onto the G1-MD is differed and showed a priority to Pb^{2+} ion. The concentration of Pb^{2+} ion was significantly decreased within the first 30 min and reached equilibrium within 2 hours, while the other metal ions decreased less than the removal ratio of 0.1.

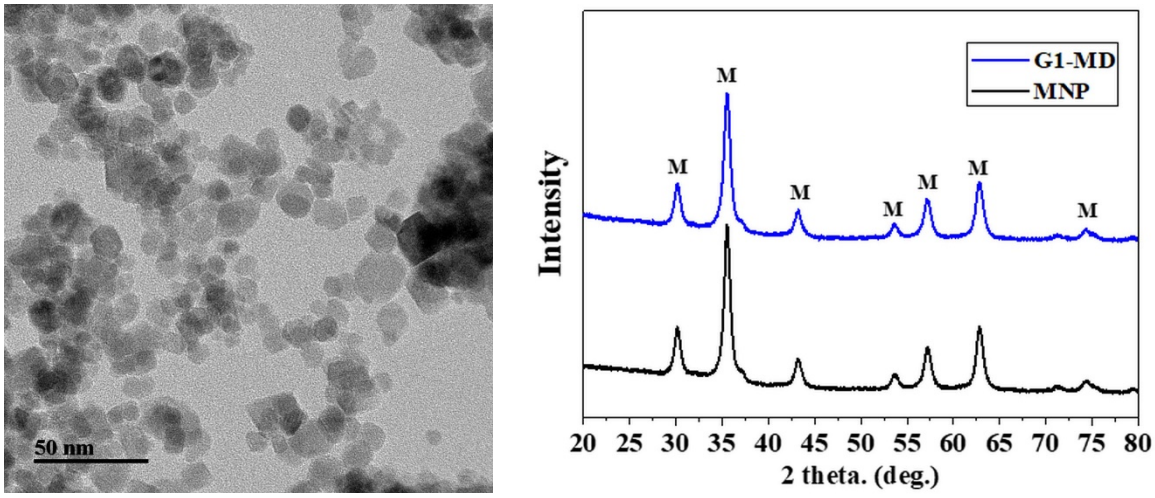

(a) (b)

Figure 1. TEM image of G1-MD and XRD peaks of MNP and G1-MD.

(a)

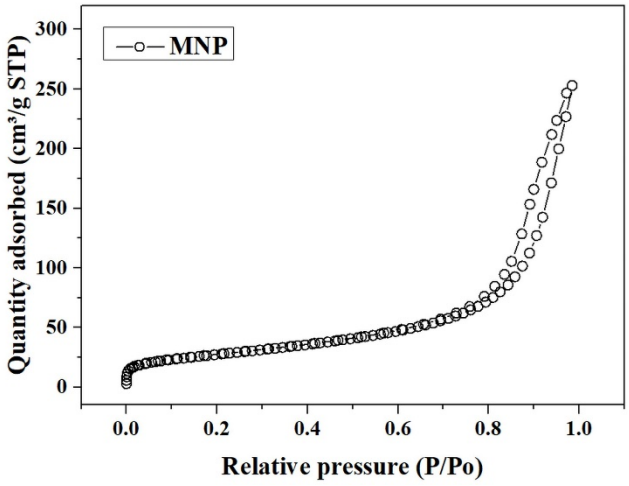

(b)

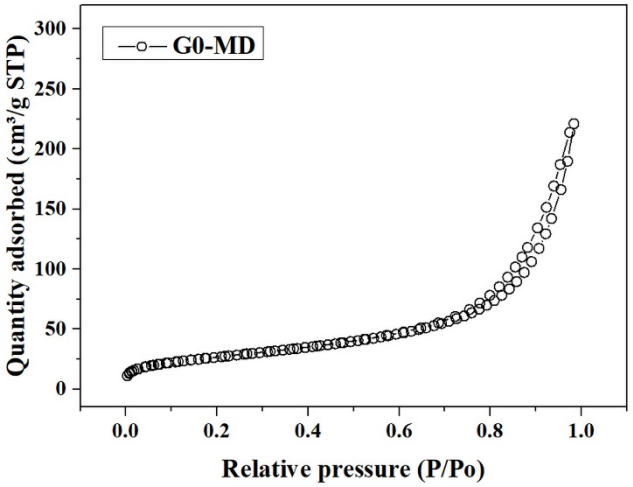

(c)

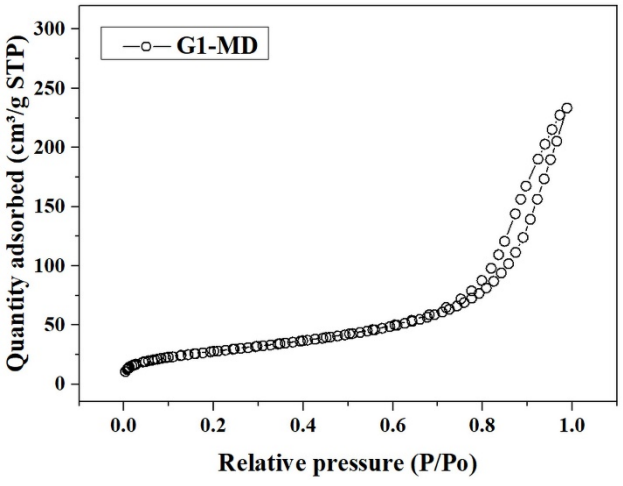

Figure 2. Nitrogen adsorption–desorption hysteresis loops on (a) MNP, (b) G0-MD, and (c) MD.

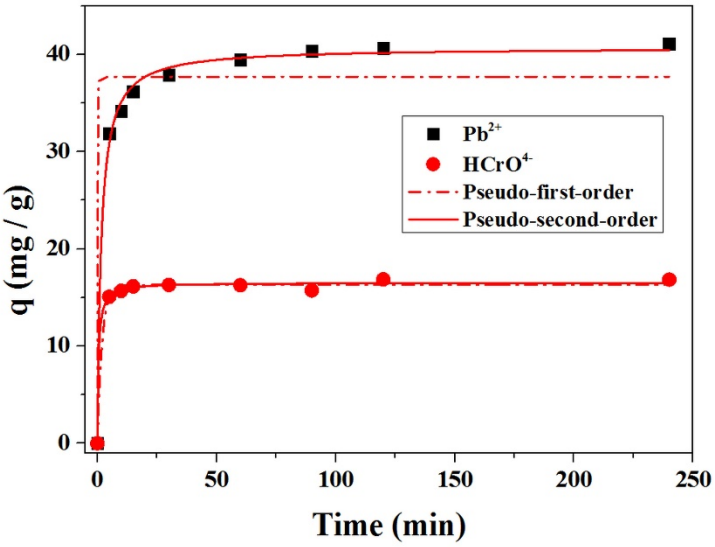

Figure 3. Kinetics of Pb^{2+} and $HCrO_4^-$ adsorption to G1-MD.

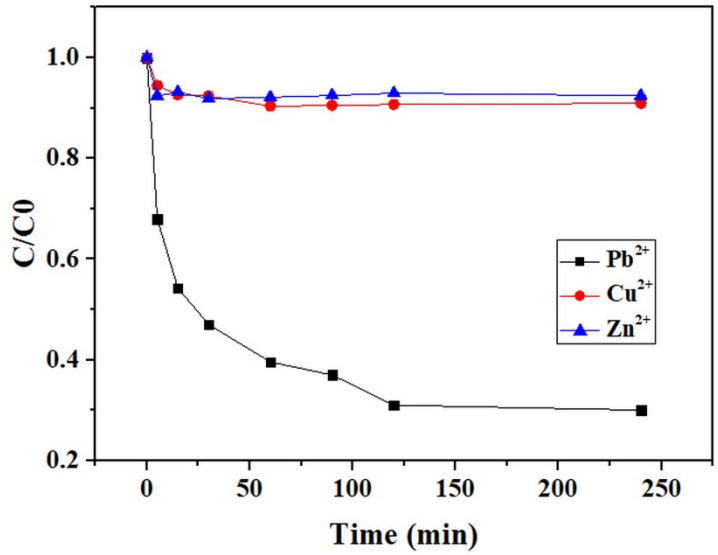

Figure 4. Kinetics of Pb^{2+}, Cu^{2+}, and Zn^{2+} in comparative condition.

2.7. Density functional theory

The DFT calculation used to explain the intermolecular bonds formed between the functional groups of the dendrimer and metal ions. The three possible configurations of single ion and one configuration of the pair of ions were proposed in figure 5. Coordination by 4 neighbors is corresponding with terminal positions of the branches of G1-MD (figure 5 (a, b, d)), and coordination by 6 neighbors with an inner position between two branches (figure 5 (c)). Each position were demonstrated after the optimization of atomic position. Calculated enthalpy of heavy metal binding was demonstrated in table 1. The experimental and theoretical calculation are well-coincided in the adsorption affinity of four heavy metal species. Since the calculated enthalpy for configuration (a) and (b) shows is lower than the others, the Pb^{2+} ion is likely coordinated with the outer part of the branches of G1- MD.

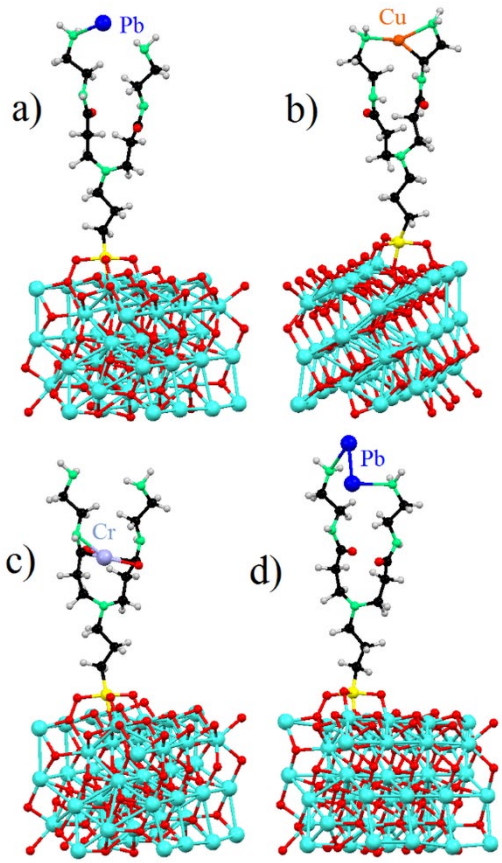

Figure 5. Optimized atomic structure of the adsorption of single (a-c) and pairs of ions of selected various metals in different position on dendritic structure on Fe_3O_4 surface.

Table 1. Langmuir isotherm parameters of MD and adsorption enthalpy in four different configurations (in figure 5).

Heavy metals	Q_m (mg/g)	K_L (mg/L)	R^2	Adsorption enthalpy (eV/ion)			
				a	b	c	d
Pb^{2+}	63.63	5.12 E-2	0.98	-1.93	-1.01	+2.01	-0.46
Cu^{2+}	14.64	5.61 E-2	0.99	+1.86	+1.02	+0.13	+1.35
Zn^{2+}	16.52	1.87 E-1	0.98	+1.73	+1.13	+2.46	+0.60
$HCrO_4^-$	24.10	8.24 E-2	0.98	-0.34	-0.26	-0.85	+0.72

3. Conclusion

Generally, the wastewater contains various kind of metal contaminants, so the theoretical approaches about the binding priority to a different kind of heavy metal is a worthwhile subject to investigate. In this work, we synthesized G1-MD and described with TEM, XRD, and BET analysis. The prepared G1-MD shows different binding affinity to four different heavy metal ions. The binding capacities onto G1-MD shows following order: Pb^{2+} > $HCrO_4^-$ > Zn^{2+} > Cu^{2+}. The G1- MD shows excellent binding performance for Pb^{2+} and $HCrO_4^-$ with maximum adsorption capacities of 63.64mg g^{-1} and 24.10 mg g^{-1}, respectively. From the DFT calculation method, most preferred binding geometries of heavy metals onto G1- MD were suggested. The experimental results show good agreement with the calculated enthalpy. Also, the adsorption energy values indicate that the terminal site of the branches are likely bound to the metal ions since the interior site appeared repulsion force for Pb^{2+} adsorption. On the other

hand, Zn^{2+} cannot form a stable bond on outer position due to its small ion radius. The adsorption capacity was related more to the number of sorptive sites than the specific surface area, which was obtained from BET analysis. In the mixed solution of heavy metal ions, the binding preference was clearly observed with Pb^{2+} adsorption onto G1-MD. It is expected that understanding the binding interfaces between the G1-MD and each different ion will help establish the basis for the application of MD, and also establish a vast potential and a wide range of environmental applications.

Acknowledgments
This study was supported by the Basic Science Research Program through the National Research Foundation of Korea (NRF) funded by the Ministry of Science, ICT and Future Planning (NRF-2018R1A2A1A05023555).

References
[1] Tomalia D A and Fréchet J M J 2002 *J. Polym. Sci. Pol. Chem.* **40** 2719
[2] Buhleier E Wehner W and Vögtle F 1978 *Chemischer Informationsdienst* **9**
[3] Newkome G R Yao Z Baker G R and Gupta V K 1985 *J. Org. Chem.* **50** 2003
[4] Kim K J and Park J W 2017 *J. Mater. Sci*. **52** 843
[5] Kim H R Jang J W and Park J W 2016 *J. Hazard. Mater.* **317** 608
[6] Jung J J Jang J W and Park J W 2016 *J. Ind. Eng. Chem.* **44** 52
[7] Tajabadi M Khosroshahi M E and Bonakdar S 2013 *Colloid Surf. A-Physicochem. Eng. Asp.* **431** 18
[8] Aziz H A Adlan M N and Ariffin K S 2008 *Bioresour. Technol.* **99** 1578
[9] Mason S E Corum K W and Ramadugu S K 2015 *Surf. Sci*. **631** 48
[10] José M S Emilio A Julian D G Alberto G Javier J Pablo O, and Daniel S P 2002 *J. Phys.-Condes. Matter* **14** 2745
[11] Kruk M and Jaroniec M 2001 *Chem. Mat.* **13** 3169
[12] Sing K S W 1985 *Pure Appl. Chem.* **603**